

Joint Optimization of Multimodal Transit Frequency and Shared Autonomous Vehicle Fleet Size with Hybrid Metaheuristic and Nonlinear Programming

Max T.M. Ng

Northwestern University Transportation Center, 600 Foster Street, Evanston, IL 60208, USA

maxng@u.northwestern.edu

Hani S. Mahmassani*

Northwestern University Transportation Center, 600 Foster Street, Evanston, IL 60208, USA

masmah@northwestern.edu

Draco Tong

Northwestern University Transportation Center, 600 Foster Street, Evanston, IL 60208, USA

draco.tong@northwestern.edu

Ömer Verbas

Argonne National Laboratory, Lemont, IL 60439, USA

omer@anl.gov

Taner Cokyasar

Argonne National Laboratory, Lemont, IL 60439, USA

tcokyasar@anl.gov

* Corresponding author

Abstract: This paper presents an optimization framework for the joint multimodal transit frequency and shared autonomous vehicle (SAV) fleet size optimization, a problem variant of the transit network frequency setting problem (TNFSP) that explicitly considers mode choice behavior and route selection. To address the non-linear non-convex optimization problem, we develop a hybrid solution approach that combines metaheuristics (particle swarm optimization, PSO) with local nonlinear programming (NLP) improvement, incorporating approximation models for SAV waiting time, multimodal route choice, and mode choice. Applied to the Chicago metropolitan area, our method achieves a 33.3% increase in transit ridership.

Keywords: transit network frequency setting problem, shared autonomous vehicles, multimodal transit, particle swarm optimization, nonlinear programming

A previous version is under review for the Conference on Advanced Systems in Public Transport and TransitData 2025 in Kyoto, Japan on 1 - 4 July 2025.

1. INTRODUCTION

1.1. Motivation

The integration of Shared Autonomous Mobility Services (SAMS) with traditional transit has emerged as a promising direction for improving system performance and service attractiveness (Ng et al., 2024b). While shared autonomous vehicles (SAVs) offer potential solutions for first/last-mile connectivity and service coverage in low-density areas, they present a fundamental question for transit agencies: whether to enhance existing transit services or replace them with SAV-based solutions. This research addresses this decision-making process

by developing an optimization framework for joint transit frequency and SAV fleet size planning.

Previous research efforts investigated the joint design of multimodal transit and SAMS in pattern frequency and SAV fleet size (Pinto et al., 2020). However, existing approaches often struggle with computational tractability when applied to large-scale networks due to the complex interactions between variables and the non-linear, non-convex problem nature. There is a critical need for efficient optimization methods that can handle city-scale transit networks while capturing the interdependencies between traditional transit services and SAMS operations.

1.2. Problem Description

This study focuses on the tactical optimization of transit pattern frequency and SAV feeder fleet size given a set of transit patterns (routes) and origin-destination (O-D) demand. We formulate this as a variant of the transit network frequency setting problem (TNFSP) with three key aspects. First, the primary objective is to maximize transit ridership (including both direct transit usage and transit with SAMS first-mile-last-mile feeders) under budget constraints across multiple time periods. Second, we also optimize SAV feeder fleet size and consider mode choice across transit (and SAMS feeders), point-to-point SAMS, and driving. Third, we allow for the strategic removal of transit routes by setting frequencies to zero, enabling resource reallocation to more efficient services (similar to Pinto et al., 2020).

The problem's complexity stems from multiple sources: the combinatorial nature of frequencies across patterns, non-linear relationships between waiting time and vehicle requirements, and the inherent non-convexity introduced by mode and route choice models. Relying on random walks to arrive at a meaningful solution alone in the high-dimensional highly non-convex solution space would require excessive computationally heavy iterations. To address these challenges, we develop an efficient solution framework that combines metaheuristics (particle swarm optimization, PSO) with local nonlinear programming (NLP) optimization, effectively exploring the complex non-convex solution space while ensuring local optimality.

The framework, as summarized in Figure 1, incorporates three approximation components to model rider interaction with transit design efficiently without relying on full agent-based simulation: (1) analytical methods for SAMS performance approximation based on fleet size and demand patterns, (2) a multimodal mode choice model using a multinomial logit framework, and (3) traveler assignment approximation with a multimodal transit network. This integrated approach enables practical application to large-scale urban transit systems while maintaining computational efficiency.

1.3. Contributions

This research makes several contributions to transit planning and optimization. Methodologically, we introduce a hybrid solution approach that combines metaheuristics (PSO) with local NLP optimization, while approximating SAMS performance, route choice, and mode choice within the optimization framework. The empirical significance is demonstrated through a case study in the Chicago metropolitan area transit network. This real-world application provides insights for transit agencies facing decisions about SAV integration and service planning. The results offer practical guidance for balancing traditional transit services with

emerging autonomous vehicle technologies, while considering operational constraints and user preferences.

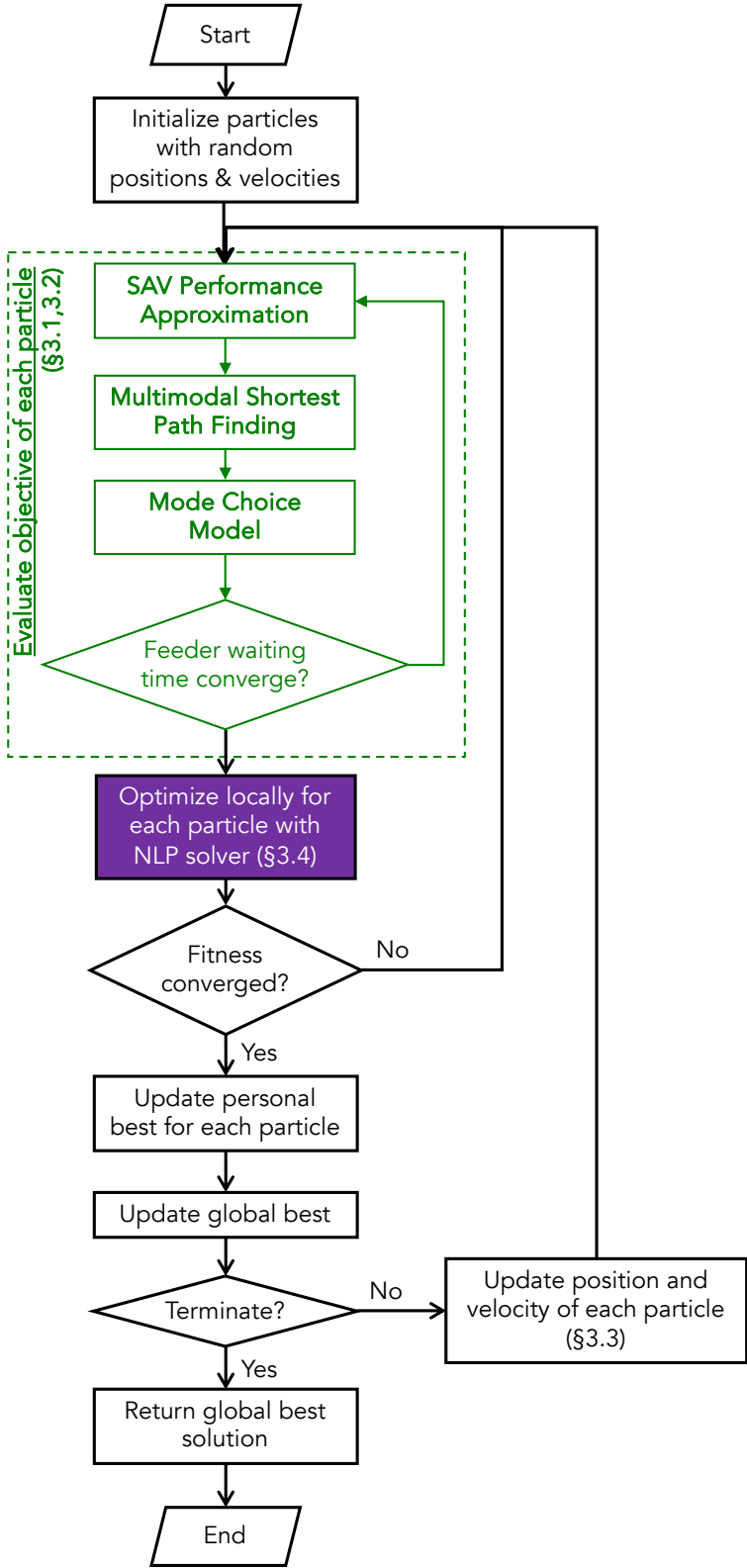


Figure 1. Flowchart of the solution approach.

The remainder of this paper is organized as follows. Section 2 reviews the relevant literature in TNFSP, SAMS, and multimodal transit. Section 3 introduces the formulation, followed by the experiment and results in Section 4 before concluding remarks in Section 5.

2. BACKGROUND

2.1. Transit Network Frequency Setting Problem (TNFSP)

The TNFSP focuses on frequency optimization and fleet assignment assuming a fixed network design, usually to minimize waiting times for passengers (see reviews by Ceder, 2016; Ibarra-Rojas et al., 2015; Durán-Micco and Vansteenwegen, 2022). Analytical approaches (e.g., Newell, 1971), heuristics (e.g., Furth and Wilson, 1981), and empirical analysis (Ceder, 1984) were preferred solutions earlier for computational limitations. Verbas and Mahmassani (2013) maximizes ridership and wait time savings using NLP, later extended to incorporate spatial and temporal demand variations and incorporating spatially and empirically-derived elasticities (Verbas et al., 2015a; Verbas and Mahmassani, 2015).

Recent developments have expanded the problem scope. Apart from the typical transit network design and frequency setting problem, features include flow assignment (Martínez et al., 2014), pricing (Bertsimas et al., 2020), schedule setting with bounded stochastic user equilibrium (Jiang et al., 2022), line planning problem (Zhou et al., 2021; Schmidt and Schöbel, 2024), and pattern generation (Ng et al., 2025b). Methodology comprises mixed integer programming (Martínez et al., 2014; Gkiotsalitis and Cats, 2022; Ng et al., 2025b), piecewise linear approximation of waiting time (Zhou et al., 2021), and metaheuristics (Aksoy and Mutlu, 2024; Martínez et al., 2014; see broader reviews by Iliopoulou et al., 2019).

This study focuses on the problem in an instance too large for exact methods (e.g., 274 patterns in Chicago). Built on the previous study (Pinto et al., 2020) that allows frequency to set to minimal for elimination, we develop an efficient solution that combines metaheuristics (PSO) with NLP for local improvement.

2.2. Shared Autonomous Mobility Service and Multimodal Transit Network

Pinto et al. (2020) established a framework for joint optimization of transit network design and shared autonomous fleet size. Other works studied SAVs as point-to-point ride-pooling services (Levin et al., 2019; Militão and Tirachini, 2021), semi-on-demand feeders (Ng et al., 2024a), or replacement of transit lines (Mo et al., 2021; Ng and Mahmassani, 2022). Previous solutions to the joint design problem of frequency and demand-responsive feeders include analytical approaches (Liu and Ouyang, 2021) and mathematical programming (Luo et al., 2021).

The complexity of SAV operations has led to significant research on fleet management and routing strategies (with seminal works: Alonso-Mora et al., 2017; Hyland and Mahmassani, 2018; see broader reviews by Narayanan et al., 2020). Agent-based simulation tools were used to identify service areas and performance of these SAVs as feeders (Ng et al., 2025a).

Our work advances the state-of-the-art beyond previous solution (Pinto et al., 2020) in three key aspects: (1) direct optimization of ridership through efficient exploration of solution space, (2) integration of mode choice in the local optimization, and (3) computationally efficient approximation methods for large-scale applications. This positioning addresses the growing need for efficient methodologies to optimize multimodal transit systems in the era of SAVs.

3. MODEL

The problem incorporates transit service frequency setting for fixed-route patterns, SAV fleet size determination for first/last mile connectivity, integration of mode choice and route selection behavior. The objective is to maximize transit ridership while considering mode choice behavior, route selection, and operational constraints across multiple time periods.

The notation is listed in Table 1. Sets are denoted as capital scripted characters (e.g., \mathcal{K} and \mathcal{L}_{pk}^χ), constants as Greek or capital Roman characters (e.g., γ^χ and T_p^ψ), and indices and variables as small Roman characters (e.g., w_k and f_{pk}). Superscripts are qualifiers and subscripts are indices. The cardinality of set \mathcal{P} is denoted $|\mathcal{P}|$.

Three modes are considered: (1) transit mode (direct or with first-mile-last-mile SAMS feeders), (2) point-to-point SAMS, and (3) driving. All demand, cost, and measurement variables are expressed per hour unless noted otherwise.

Table 1. Notation.

<i>Sets and indices</i>	
\mathcal{K}	Time period, indexed by $k \in \mathcal{K}$
\mathcal{N}	Set of nodes in network, indexed by $o, d \in \mathcal{N}$
\mathcal{P}	Set of transit patterns, indexed by $p \in \mathcal{P}$
\mathcal{M}	Set of transit modes, indexed by $m \in \mathcal{M}$
m_p	Transit mode used by pattern $p \in \mathcal{P}$
\mathcal{L}	Set of links in network, indexed by $l \in \mathcal{L}$
\mathcal{L}_{pk}^χ	Set of SAMS feeder links used to access pattern $p \in \mathcal{P}$ in period $k \in \mathcal{K}$, $\mathcal{L}_{pk}^\chi \subset \mathcal{L}$
\mathcal{L}_{pk}^τ	Set of transit links of pattern $p \in \mathcal{P}$ in period $k \in \mathcal{K}$, $\mathcal{L}_{pk}^\tau \subset \mathcal{L}$
<i>Parameters</i>	
A_1, A_2	Cut-off utilization in SAMS feeder waiting time piecewise linear function
B_m	Vehicle size of mode $m \in \mathcal{M}$
C_{odk}^τ	Transit fare from $o \in \mathcal{N}$ to $d \in \mathcal{N}$ in period $k \in \mathcal{K}$
D_k	Duration of time period $k \in \mathcal{K}$
F_p^+	Maximum policy frequency for pattern $p \in \mathcal{P}$
Q_{odk}	Demand from $o \in \mathcal{N}$ to $d \in \mathcal{N}$ in period $k \in \mathcal{K}$
S_k^+	Maximum SAMS feeder fleet size for period $k \in \mathcal{K}$
T_p^ψ	Cycle time of pattern $p \in \mathcal{P}$ (in hour)
T_l^χ	Journey time of SAMS feeder link $l \in \mathcal{L}_{pk}^\chi, p \in \mathcal{P}, k \in \mathcal{K}$
U_{odk}^σ	Utility of point-to-point SAMS for traveling from $o \in \mathcal{N}$ to $d \in \mathcal{N}$ in period $k \in \mathcal{K}$
U_{odk}^δ	Utility of driving for traveling from $o \in \mathcal{N}$ to $d \in \mathcal{N}$ in period $k \in \mathcal{K}$
W	Minimum average traveler wait time for SAMS feeders
α_1, α_2	SAMS feeder waiting time fixed-point iterations step sizes for calculation / approximation
β_0^τ	Mode-specific constant for transit
β_1, β_2	Coefficient for travel time / fare in utility
δ	SAMS feeder waiting time fixed-point iterations convergence threshold
Δ_1, Δ_2	Slopes of SAMS feeder waiting time piecewise linear function

γ_m^τ	Unit operating cost of transit mode $m \in \mathcal{M}$ (in \$ per vehicle-hour)
γ^χ	Unit operating cost of SAMS (in \$ per vehicle-hour)
Γ^o	Daily operating budget
Decision variables	
f_{pk}	Transit frequency of pattern $p \in \mathcal{P}$ in period $k \in \mathcal{K}$
s_k	SAV fleet size in period $k \in \mathcal{K}$
Auxiliary variables	
q_l^λ	Transit demand on link $l \in \mathcal{L}$
q_{odk}^τ	Transit demand from $o \in \mathcal{N}$ to $d \in \mathcal{N}$ in period $k \in \mathcal{K}$
r_{pk}^τ	Transit boarding rejection for pattern $p \in \mathcal{P}$ in period $k \in \mathcal{K}$
r_{pk}^χ	SAMS feeder boarding rejection for pattern $p \in \mathcal{P}$ in period $k \in \mathcal{K}$
u_{odk}^τ	Utility of transit (with SAMS feeders) for traveling from $o \in \mathcal{N}$ to $d \in \mathcal{N}$ in period $k \in \mathcal{K}$
t_{odk}^τ	Transit journey time from $o \in \mathcal{N}$ to $d \in \mathcal{N}$ in period $k \in \mathcal{K}$
w_k	Average SAMS feeder waiting time in period $k \in \mathcal{K}$
ρ_k	SAMS fleet utilization rate in period $k \in \mathcal{K}$
Functions	
$G(f, u)$	A multimodal graph based on transit frequency f and SAMS feeder waiting time u
$SP(G)$	Shortest path journey time in a multimodal graph G
Additional sets in local sub-problem	
\mathcal{L}_{odk}^ϕ	Links involved in the shortest path from $o \in \mathcal{N}$ to $d \in \mathcal{N}$ in period $k \in \mathcal{K}$
\mathcal{P}_{odk}^ϕ	Patterns involved in the shortest path from $o \in \mathcal{N}$ to $d \in \mathcal{N}$ in period $k \in \mathcal{K}$
\mathcal{R}_{pk}	Set of OD pairs that use pattern $p \in \mathcal{P}$ in the shortest paths in period $k \in \mathcal{K}$, $\mathcal{R}_{pk} \subset \mathcal{N} \times \mathcal{N}$
Additional parameters in local sub-problem	
F_{pk}	Reference frequency for pattern $p \in \mathcal{P}$ in period $k \in \mathcal{K}$
N_{odk}^χ	Number of SAMS links involved in shortest path from $o \in \mathcal{N}$ to $d \in \mathcal{N}$ in period $k \in \mathcal{K}$ from approximation models; $N_{odk}^\chi \in \{0,1,2\}$
Q_{odk}^τ	Reference transit demand from $o \in \mathcal{N}$ to $d \in \mathcal{N}$ in period $k \in \mathcal{K}$ from approximation models
Q_{pk}^π	Reference peak demand from $o \in \mathcal{N}$ to $d \in \mathcal{N}$ in period $k \in \mathcal{K}$ from approximation models
T_{odk}^χ	SAMS feeder time used in the shortest path from $o \in \mathcal{N}$ to $d \in \mathcal{N}$ in period $k \in \mathcal{K}$
U_k	Reference SAMS waiting time in period $k \in \mathcal{K}$
U^+	Maximum SAMS waiting time
Y^-, Y^+	Lower/upper bound of demand elasticity
ε	Objective convergence threshold
λ_i	Regularization parameter, $i = 0,1,2$
γ^ω	Waiting disutility factor
Additional auxiliary variables in local sub-problem	
q_{pk}^ϕ	Transit demand for pattern $p \in \mathcal{P}$ in period $k \in \mathcal{K}$
y_{pk}^τ	Transit demand elasticity factor for pattern $p \in \mathcal{P}$ in period $k \in \mathcal{K}$
y_{pki}^χ	SAMS demand elasticity factor for pattern $p \in \mathcal{P}$ in period $k \in \mathcal{K}$ with $i \in \{1,2\}$ SAMS links

<i>Additional sets in metaheuristics</i>	
\mathcal{E}	Sets of epochs, indexed by $e \in \mathcal{E}$
\mathcal{J}	Sets of particles, indexed by $i \in \mathcal{J}$
<i>Additional parameters in metaheuristics</i>	
P_i	Particle swarm optimization hyperparameters, $i = 0,1,2$
<i>Additional auxiliary variables in metaheuristics</i>	
h_i	Random variables for particle swarm optimization velocity, $i = 1,2$
$x_{e,i}$	Solution of particle $i \in \mathcal{J}$ in epoch $e \in \mathcal{E}$
$\widehat{x}_{e,i}$	Individual best solution achieved by particle $i \in \mathcal{J}$ until epoch $e \in \mathcal{E}$
x_e^*	Global best solution until epoch $e \in \mathcal{E}$
$v_{e,i}$	Velocity of particle $i \in \mathcal{J}$ in epoch $e \in \mathcal{E}$

3.1. Mathematical Formulation

The overall objective is to maximize served demand (demand q_{odk}^τ minus boarding rejections of transit r_{pk}^τ and SAMS feeder r_{pk}^χ) in Eq. (1) across multiple periods $k \in \mathcal{K}$.¹ The decision variables are f_{pk} bounded by policy frequencies in Eq. (2) and SAMS feeder fleet size s_k bounded by fleet availability in Eq. (3).

$$\max_{f_{pk}, s_k} \sum_{k \in \mathcal{K}} \sum_{o, d \in \mathcal{N}} q_{odk}^\tau - \sum_{k \in \mathcal{K}} \sum_{p \in \mathcal{P}} \max(r_{pk}^\tau, r_{pk}^\chi) \text{ s.t. (2)-(12)} \quad (1)$$

$$0 \leq f_{pk} \leq F_p^+, \forall p \in \mathcal{P}, k \in \mathcal{K} \quad (2)$$

$$0 \leq s_k \leq S_k^+, \forall k \in \mathcal{K} \quad (3)$$

The transit ridership q_{odk}^τ is determined through a multinomial logit mode choice model incorporating utility functions for transit u_{odk}^τ , point-to-point SAMS U_{odk}^σ , and driving U_{odk}^δ in Eq. (4). The utilities are calculated as the sum of alternative-specific constants (ASCs) β_0^τ , travel time t_{odk}^τ weighted by β_1 , and fare C_{odk}^τ weighted by β_2 , such as for transit as shown in Eq. (5).

$$q_{odk}^\tau = Q_{odk} \frac{\exp(u_{odk}^\tau)}{\exp(u_{odk}^\tau) + \exp(U_{odk}^\sigma) + \exp(U_{odk}^\delta)}, \forall o, d \in \mathcal{N}, k \in \mathcal{K} \quad (4)$$

$$u_{odk}^\tau = \beta_0^\tau + \beta_1 t_{odk}^\tau + \beta_2 C_{odk}^\tau, \forall o, d \in \mathcal{N}, k \in \mathcal{K} \quad (5)$$

The transit journey time t_{odk}^τ is based on the shortest path in Eq. (6) in a multimodal graph $G(f_{pk}, w_k)$, in which the entry arc costs represent the waiting times based on transit frequency f_{pk} and SAMS feeder waiting time w_k . The details are discussed in Section 3.2.

$$t_{odk}^\tau = SP \left(G(f_{pk}, w_k) \right), \forall o, d \in \mathcal{N}, k \in \mathcal{K} \quad (6)$$

The SAMS feeder waiting time w_k is approximated through a piecewise linear function of utilization ρ_k in Eq. (7) as illustrated in Figure 2 (Pinto et al., 2020). The utilization is calculated with the total SAMS feeder time (sum of flows q_l^λ and times T_l^χ of SAMS links \mathcal{L}_{pk}^χ) per total

¹ This framework has the potential for future expansion to incorporate time-dependent scenarios and transit frequency hyperpaths.

vehicle capacity (fleet size s_k multiplied by average occupancy R^σ) in Eq. (8). The SAMS feeder flow is output from the trip assignment of the multimodal graph in Eq. (9).

$$w_k = \begin{cases} W, \rho_k \leq A_1 \\ W + \Delta_1(\rho_k - A_1), A_1 < \rho_k \leq A_2 \\ W + \Delta_1(A_2 - A_1) + \Delta_2(\rho_k - A_2), \rho_k > A_2 \end{cases}, \forall k \in \mathcal{K} \quad (7)$$

$$\rho_k = \frac{\sum_{p \in \mathcal{P}} \sum_{l \in \mathcal{L}_{pk}^\chi} q_l^\lambda T_l^\chi}{R^\sigma s_k}, \forall k \in \mathcal{K} \quad (8)$$

$$q_l^\phi = TAP(G(f_{pk}, w_k), q_{odk}^\tau), \forall l \in \mathcal{L}, k \in \mathcal{K} \quad (9)$$

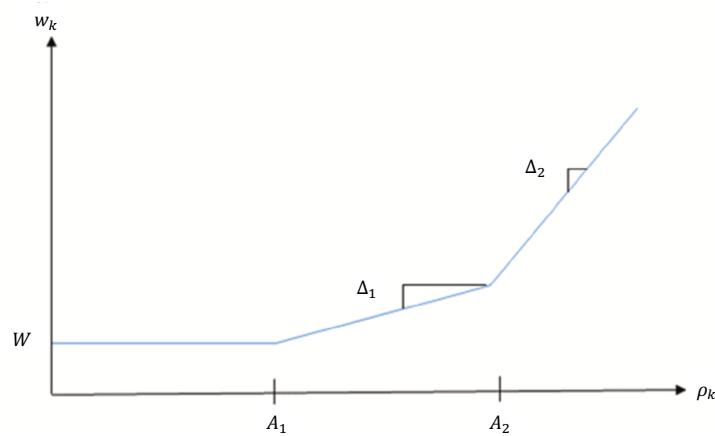


Figure 2. Piecewise linear relationship between average SAMS feeder wait time (w_k) and estimated SAMS fleet utilization rate (ρ_k).

The boarding rejections are calculated based on the peak transit flow for each pattern and SAMS feeders. In Eq. (10), the transit rejection r_{pk}^τ is the peak flow minus the pattern capacity (vehicle capacity B_{m_p} multiplied by frequency). In Eq. (11), the SAMS feeder rejection r_{pk}^χ is the sum of feeder flows multiplied by the unserved utilization $(1 - 1/\rho_k)$.

$$r_{pk}^\tau = \max\left(0, \max_{l \in \mathcal{L}_{pk}^\tau} q_l^\lambda - B_{m_p} f_{pk}\right), \forall p \in \mathcal{P}, k \in \mathcal{K} \quad (10)$$

$$r_{pk}^\chi = \max\left(0, \left(1 - \frac{1}{\rho_k}\right) \sum_{l \in \mathcal{L}_{pk}^\chi} q_l^\lambda\right), \forall p \in \mathcal{P}, k \in \mathcal{K} \quad (11)$$

Finally, the daily budget constraint² for all period (each with duration of D_k) is set in Eq. (12) by estimating the transit cost with the unit cost $\gamma_{m_p}^\tau$, cycle time T_p^ψ , and frequency, and the SAMS feeder costs with unit cost γ^χ and the fleet size.

² Different operating budgeting can be considered with the formulation, e.g., fares or capital costs. The unit operating costs are used here for illustration.

$$\sum_{k \in \mathcal{K}} D_k \left(\sum_{p \in \mathcal{P}} \gamma_{m_p}^{\tau} T_p^{\psi} f_{pk} + \gamma^{\chi} s_k \right) \leq \Gamma^o \quad (12)$$

3.2. Approximation Models

To model rider behavior efficiently without full agent-based simulation, we implement three key approximation components: SAMS performance approximation for feeder waiting time in Eq. (7), multimodal graph for route choice in Eq. (6) and (9), and multinomial logit model mode choice in Eq. (4).³ This subsection discusses the implementation of the multimodal graph and SAMS performance approximation in detail.

The multimodal directed graph $G(f_p, w)$ (illustrated in Figure 3) handles route choice for transit journey time and graph loading for peak transit load and SAMS feeder demand. It comprises demand nodes and transit nodes, connected by three types of edges: (1) Access edges (walking/feeder) connecting demand and transit nodes, with access⁴ and waiting costs; (2) Transit edges connecting transit nodes of each pattern with the travel time as cost; and (3) Transfer edges connecting transit nodes of different patterns with transfer penalty and waiting as cost. Additionally, factors are applied to penalize walking, waiting and transfers.

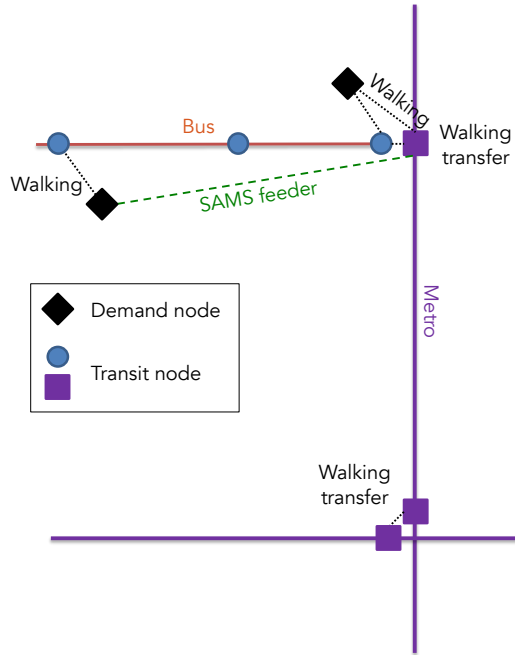


Figure 3. Illustration of multimodal graphs.

After construction, the graph edge costs are updated in each iteration with new frequency f_{pk} and SAMS waiting times w_k for each period k . The shortest path is then found for each O-D pair to compute the weighted transit journey time and load the graph to calculate the peak traffic flow.

³ The framework is compatible with agent-based simulation tools, e.g., NU-TRANS (Verbas et al., 2015b), POLARIS (Auld et al., 2016), and FleetPy (Engelhardt et al., 2022), to replace each approximation model for desired accuracy and allowed computation time.

⁴ The access costs are approximated with constant walking speed for walking edges, and with constant speed, detour, and occupancy for feeder edges.

For SAMS feeder performance approximation, the waiting time w_k for a given demand has no closed-form solution due to its circular dependency with the route and mode choice. To speed up convergence and minimize graph operations required, we employ fixed-point iterations enhanced by analytical approximations:

1. Assume initial SAMS feeder waiting time w_k for graph construction.
2. Update total SAMS feeder demand q_i^λ based on trip assignment of the multimodal graph $G(f_{pk}, w_k)$ in Eq. (9).
3. Calculate utilizations ρ_k in Eq. (8) and resulting SAMS waiting times \widetilde{w}_k in Eq. (7).
4. Approximate new SAMS feeder waiting time \widehat{w}_k with fixed-point iterations using \widetilde{w}_k as starting point and considering demand elasticities, i.e., Eq. (7) and $\widehat{\rho}_k \propto \exp(\beta_1 \gamma^w (\widehat{w}_k - w_k))$, $\forall k \in \mathcal{K}$.
5. Set new SAMS waiting time with a step size between the values from calculation (Step 3) and approximation (Step 4), i.e., $w'_k = \alpha_1 \widehat{w}_k + \alpha_2 \widetilde{w}_k$.
6. Go to Step 2 if $|w'_k - w_k| > \delta$; otherwise end.

3.3. Metaheuristics

The solution methodology combines global exploration through metaheuristics (PSO) (Kennedy and Eberhart, 1995)⁵ with local improvement via NLP. This hybrid structure solves the non-convex non-linear optimization problem with the computationally heavy shortest path update and network loading. The approach can be interpreted from two perspectives: as a metaheuristic framework using local NLP optimization as a repair operator, or as NLP optimization with PSO-guided multi-starts.

The need for global search in this problem arises from several factors that create a highly complex, non-convex solution space:

- The combinatorial nature of frequency settings across hundreds of transit patterns;
- The circular dependency between transit service levels, SAV fleet size, and resulting demand;
- The non-linear relationships in mode choice and waiting time functions; and
- The presence of multiple local optima due to network effects and demand interactions.

These characteristics render it unlikely to find high-quality solutions through local search alone, necessitating a global exploration strategy. The solution space topology varies significantly depending on the specific problem instance, network structure, and demand patterns.

In this implementation, we utilize PSO as the global search component, though the framework is flexible and can accommodate other metaheuristics. The key aspect is the combination of global exploration with local NLP improvement, where the metaheuristic guides the search to promising regions that are then refined through local optimization.

For solution representation, each particle $i \in \mathcal{I}$ of epoch $e \in \mathcal{E}$ represents a complete solution vector $x_{e,i} = [f_{pk}, s_k]$, combining pattern frequencies f_{pk} and SAV fleet sizes s_k for all time periods $k \in \mathcal{K}$.⁶

⁵ PSO is chosen for its population-based stochastic optimization to explore the non-convex solution space, natural parallelization potential through independent particle evaluations, and effective representation of solution space through particle positions (frequencies and fleet sizes) and velocities.

⁶ To maintain feasibility of each solution with the budget constraint, the remaining budget after providing s_k is used to scale transit frequencies f_{pk} .

The particle movement mechanism follows standard PSO dynamics, where each particle's position is updated in Eq. (13) based on last position and velocity $v_{e+1,i}$. In Eq. (14), the velocity is set by three terms: inertia, cognitive (distance to local best solution $\widehat{x}_{e,i}$), and social (distance to global best solution x_e^*), with P_0, P_1, P_2 as hyperparameters and h_1, h_2 as random variables specific to each particle and iteration. These accelerate the particles stochastically towards personal and global best.

$$x_{e+1,i} = x_{e,i} + v_{e+1,i} \quad (13)$$

$$v_{e+1,i} = P_0 v_{e,i} + P_1 h_1 (\widehat{x}_{e,i} - x_{e,i}) + P_2 h_2 (x_e^* - x_{e,i}) \quad (14)$$

3.4. Local Sub-Problem

NLP local improvement helps to refine the solution to reduce the PSO iterations required. The local sub-problem keeps the objective of maximizing served demand (transit demand minus rejections), but focuses on modeling the parametrizable components. The key modifications include fixed shortest-path routes, local demand elasticity with respect to waiting times, and aggregation of O-D demand to pattern-level to reduce problem size.

The modified objective in Eq. (15), similar to Eq. (1), maximizes pattern-level demand q_{pk}^ϕ subtracted by boarding rejections. L2 regularization (with hyperparameter λ_0) and local bounds in Eq. (16)-(17) controls step size while improving upon F_{pk} and U_k from the previous solution.

$$\max_{f_{pk}, u_k} \sum_{k \in \mathcal{K}} \sum_{p \in \mathcal{P}} \left(q_{pk}^\phi - \max(r_{pk}^\tau, r_{pk}^\chi) - \lambda_0 (f_{pk} - F_{pk})^2 - \lambda_0 (u_k - U_k)^2 \right) \quad (15)$$

$$\text{s.t. Eq. (3),(7),(12),(16)-(24)}$$

$$0 \leq f_{pk} \leq \lambda_1 F_{pk} \leq F_p^+, \forall p \in \mathcal{P}, k \in \mathcal{K} \quad (16)$$

$$\lambda_2 U_k \leq u_k \leq U^+, \forall k \in \mathcal{K} \quad (17)$$

In Eq. (18), the pattern-level demand is aggregated from O-D level demand Q_{odk}^τ by pattern and the number of SAMS feeders used N_{odk}^χ . Elasticity factors for transit waiting time y_{pk}^τ and SAV feeder waiting time y_{pki}^χ , where $i = N_{odk}^\chi \in \{0,1,2\}$, are derived as marginal changes from the multinomial logit model⁷ from Eq. (4)-(5). This leads to the local approximations in Eq. (19)-(20), whereas β_1 and γ^ω are respectively the utility coefficient of travel time and waiting time factor. Additional bounds are imposed on the variables in Eq. (21) to facilitate numerical stability.

$$q_{pk}^\phi = y_{pk}^\tau \sum_{i=\{0,1,2\}} y_{pki}^\chi \sum_{(o,d) \in \mathcal{R}_{pk} | N_{odk}^\chi = i} Q_{odk}^\tau, \forall p \in \mathcal{P}, k \in \mathcal{K} \quad (18)$$

$$y_{pk}^\tau = \exp \left(\frac{\beta_1 \gamma^\omega}{2} \left(\frac{1}{f_{pk}} - \frac{1}{F_{pk}} \right) \right), \forall p \in \mathcal{P}, k \in \mathcal{K} \quad (19)$$

⁷ The derivation assumes insignificant changes in the logit model denominator and negligible effects of cross-pattern effects on demand. The first assumption is likely to hold with lower transit ridership relative to driving and SAMS.

$$y_{pki}^\chi = \exp(i \beta_1 \gamma^w (w_k - W_k)), \forall p \in \mathcal{P}, k \in \mathcal{K}, i \in \{0,1,2\} \quad (20)$$

$$Y^- \leq y_{pk}^\tau, y_{pki}^\chi \leq Y^+, \forall p \in \mathcal{P}, k \in \mathcal{K}, i \in \{0,1,2\} \quad (21)$$

SAMS waiting time w_k is still calculated with Eq. (7), but the utilization is now approximated in Eq. (22) with adjusted total SAMS time $Q_{odk}^\tau T_{odk}^\chi$ using previous elasticity factors.

$$\rho_k = \frac{1}{R^\sigma S_k} \sum_{p \in \mathcal{P}} y_{pk}^\tau \left[\sum_{i=\{1,2\}} y_{pki}^\chi \sum_{(o,d) \in \mathcal{R}_{pk} | N_{odk}^\chi = i} Q_{odk}^\tau T_{odk}^\chi \right], \forall k \in \mathcal{K} \quad (22)$$

In Eq. (23)-(24), transit boarding and SAMS feeder boarding rejection are calculated similar to Eq. (10)-(11), except that peak and transit demands (Q_{pk}^π, Q_{odk}^τ) are from the approximation models and adjusted by the elasticity.

$$r_{pk}^\tau = \max\left(0, y_{pk}^\tau Q_{pk}^\pi - B_{m_p} f_{pk}\right), \forall p \in \mathcal{P}, k \in \mathcal{K} \quad (23)$$

$$r_{pk}^\chi = \max\left(0, \left(1 - \frac{1}{\rho_k}\right) y_{pk}^\tau \sum_{i=\{1,2\}} y_{pki}^\chi \sum_{(o,d) \in \mathcal{R}_{pk} | N_{odk}^\chi = i} Q_{odk}^\tau\right), \forall p \in \mathcal{P}, k \in \mathcal{K} \quad (24)$$

Lastly, the budget constraint in Eq. (12) still applies.

This local sub-problem is solved with an NLP solver Knitro using interior-point/barrier direct algorithm. We adopt a multi-start strategy with local perturbations that creates new solutions locally around the old ones following a distribution. This further enhances exploration of the local solution space.

As shown in Figure 1, the local sub-problem optimization is run after and before the approximation models to evaluate the fitness and update the route and mode choices. It is re-run until the objective converges, i.e., the change magnitude is smaller than a threshold ε . This ensures sufficient exploitation before passing the solutions to metaheuristics for further exploration.

4. EXPERIMENT AND RESULTS

The model is applied to the Chicago metropolitan area transit network to demonstrate the effectiveness in a large-scale urban setting. The network configuration incorporates multiple transit modes: commuter rail (Metra), metro rail (Chicago Transit Authority, CTA), and bus services (CTA and Pace). The multimodal network is constructed with GTFS dataset. Transfer connections are established between routes within walkable distance. Access connections are set from demand zones as walking links to the closest transit modes, and SAMS feeder links to rail nodes within 5km when walking distance exceeds threshold. For the driving and point-to-point SAMS modes, the journey times and costs are estimated based on a road network extracted with OSMnx (Boeing, 2024) with congestion factors. Point-to-point SAMS also include a detour factor $\phi = 1.3$ (Ng et al., 2024b).

Three periods are considered in a day, covering peak and off-peak hours. Demand data are extracted from the activity-based demand model CT-RAMP (Chicago Metropolitan Agency for Planning, 2023). Mode choice model is applied that separates car owners and non-owners. The operating costs are the average U.S. revenue-hourly costs from the National Transit Database (Federal Transit Administration, 2021). The mode choice model and SAMS performance approximation parameters are set with reference to Pinto et al. (2020). Operating budgets are set to align with current transit agency expenditures. The coefficients of walking and waiting are set with reference to Wardman (2004). A baseline case is used to compare with the optimization results and as the initial solution for warm-starting.⁸ The parameter values are summarized in Table 2. The solution vector is of size 825.

Table 2. Input parameters of the models.

$ \mathcal{K} $	2	C_{odk}^σ	\$(4.85+0.2\text{time}+0.5\text{dist})\$	γ_m^τ	\$[4765, 2033, 188, 188]/h\$
$ \mathcal{N} $	41186	C_{odk}^δ	\$(0.54\text{dist})\$	γ^x	10min
$ \mathcal{P} $	274	F_p^+	20/h	Γ^o	\$10M/day
\mathcal{M}	[Metra rail, CTA rail, CTA bus, Pace bus]	S_k^+	10000	ε	0.1
$ \mathcal{L} $	208375	W	3min	$\lambda_0, \lambda_1, \lambda_2$	0.001, 2, 0.5
$ \mathcal{E} $	30	α_1, α_2	0.8, 0.2	U^+	60min
$ \mathcal{J} $	40	$\beta_0^\tau, \beta_0^\sigma, \beta_0^\delta$	-1.5, -1.7, 0	Y^-, Y^+	0, 3
A_1, A_2	0.5, 0.8	β_1, β_2	-0.12/min, -0.5/\$	γ^ω	1.5
B_m	[1200,1000,70,70]	δ	3min	P_0, P_1, P_2	0.9, 2.0, 2.0
C_{odk}^τ	\$2.5	Δ_1, Δ_2	20min, 50min		

The optimization was performed on a computing cluster with the Red Hat Enterprise Linux 7.9 operating system, Intel Xeon Gold 6338 2GHz, 32 cores, and 224 GB RAM with 8 threads. The solutions are implemented with Pymoo (Blank and Deb, 2020) for metaheuristics and Knitro (Byrd et al., 2006) for the NLP solver. Each PSO+NLP iteration takes around 3 hours.

4.1. Computational Performance

The hybrid PSO-NLP method demonstrates superior computational efficiency compared to PSO-only implementation as shown in Figure 4. The first PSO-NLP iteration results demonstrate the effectiveness of NLP-based local optimization, even before PSO's global search takes effect. In Figure 4a, the first iteration achieved a 24.8% increase in total served demand compared to the baseline. The PSO-NLP approach achieved rapid convergence to high-quality solutions, while traditional PSO struggled to surpass an objective of 400,000 after deviating from the initial solutions in Figure 4b. Through global exploration of the solution space, later PSO-NLP enhanced the solution at around 14th iteration, demonstrating the value of global search that provides better starting points for NLP to work on.

⁸ The peak-hour frequency in the baseline case is 4 for commuter rail, 12 for metro rail, 7 for city bus, 4 for suburban bus; non-peak frequency is 1 for commuter rail, 8 for metro rail, 5 for city bus, 2 for suburban bus.

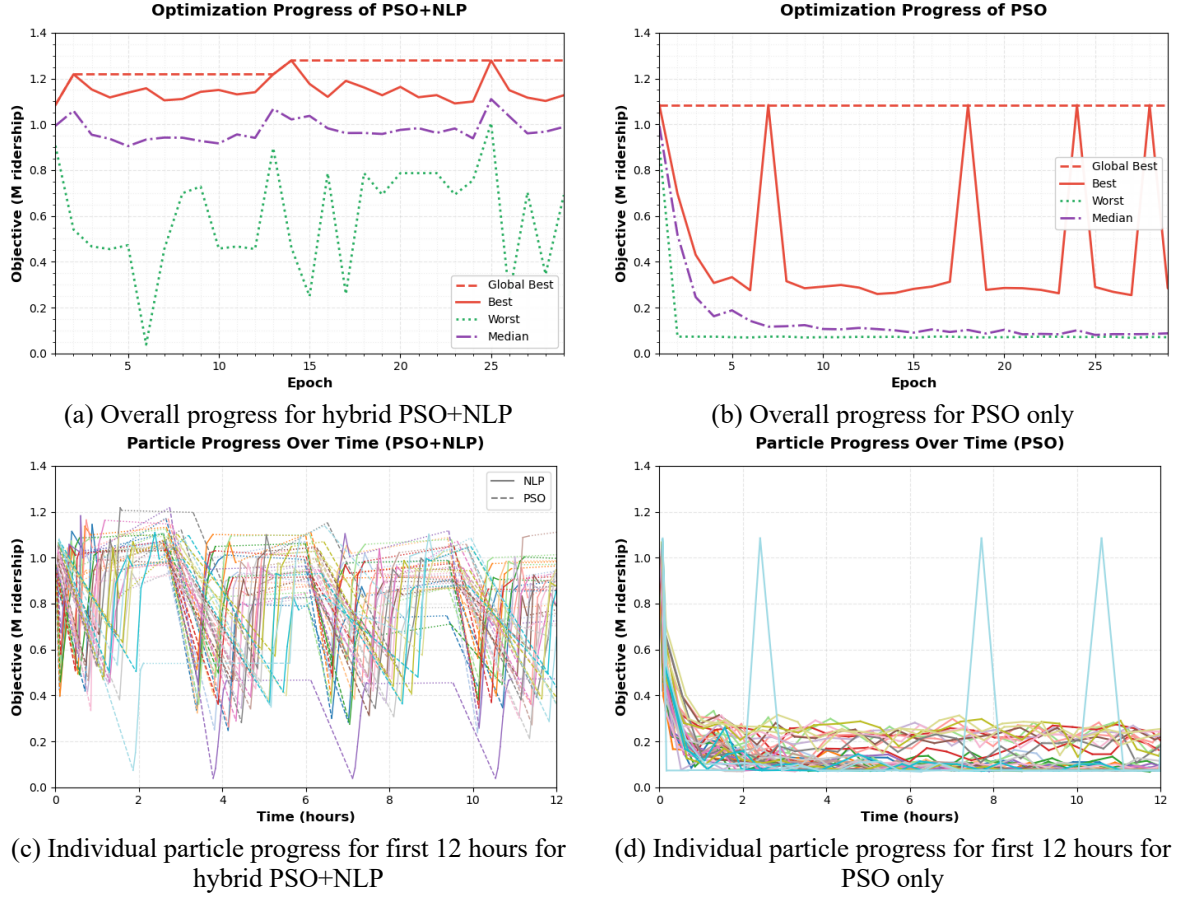


Figure 4. Optimization progress.

The combination of PSO's global exploration capabilities with NLP's local improvement mechanism is highly effective that most solutions maintain high quality after local improvement, albeit with a longer computation time required (around 95 hours compared to 12 hours of PSO alone). The individual particle trajectories (Figure 4c) show frequent local improvements through NLP while maintaining diversity through PSO. This contrasts with Figure 4d where PSO alone fails to improve solutions higher or even to the level of initial solution (except the occasional revisit to the initial solution), likely due to the highly non-convex problem nature that it is unlikely to arrive at a quality solution (reasonable combination of transit frequency and SAV fleet size) randomly.

While the NLP-approximation iterations are computationally intensive, they are essential for solution refinement. The PSO component facilitates broader exploration of the solution space, leading to the discovery of promising solution regions that were subsequently optimized by NLP. This hybrid approach maintains solution diversity while ensuring effective local optimization, resulting in more robust and higher-quality solutions compared to single-method approaches.

4.2. Solution Results

The implementation of the proposed hybrid PSO-NLP optimization framework yields significant improvements in system performance. Table 3 compares the baseline case with both the first iteration best solution (NLP-only) and the global optimal solution (PSO+NLP).

The first iteration results demonstrate the effectiveness of NLP-based local optimization, even before PSO's global search takes effect. Compared to the baseline, the first iteration achieved a 24.8% increase in total served demand while only reducing active routes by 3.3% (from 274 to 265). This shows that NLP alone can significantly improve system efficiency through service reallocation. Peak-hour served demand increased modestly by 3.9%, while off-peak served demand nearly doubled with a 97.2% increase. The service frequency adjustments in the first iteration show a clear trend of service consolidation (though less aggressive than the global best solution). Peak-hour total frequency decreased by 30.9%, with reductions across all modes and most significantly suburban bus. Off-peak services saw similar patterns but with one notable exception: suburban rail frequency increased by 15.8%, indicating the model's early recognition of rail's efficiency for off-peak service. The median route frequencies decreased slightly at peak hours (-11.1%) but increased during off-peak (6.6%), suggesting a more balanced service distribution.

The subsequent global search through PSO+NLP further improved these results. The optimal solution significantly reduced the number of active transit patterns by 60.6% from 274 to 108 with a fleet of 5,000 SAVs. This restructuring results in a 33.3% increase in total served demand despite fewer patterns used, thanks to flexibility provided by the SAVs. The ridership increase comprises a 12.2% peak-hour and 106.7% off-peak increase. This substantial improvement can be attributed to the strategic deployment of SAVs that help to expand coverage, particularly in off-peak hours where demand is not dense enough for traditional transit modes to achieve economy of scale. As for the services provided in each mode, the redesign reduces the total service frequency at peak hours (32.6%) and off-peak hours (63.5%) to reserve budget for SAV operations. Most of the frequency cut comes from suburban bus services, while other three modes see slight decrease at peak hours and suburban rail actually sees off-peak frequency improvement to attract more riders. The restructuring consolidates services and provides high frequency at major corridors, as seen from the higher median route frequency (44.3% and 61.9% increases for metro rail and bus at peak hours). The SAV feeder service contributes to 14.4% and 35.4% of trips at peak and off-peak hours respectively. This again shows that SAV feeder plays a bigger role at off-peak hours when demand is less dense. The SAV feeders are busy at peak hours with 14.4 min average waiting time, and in good service at off-peak with 5.9 min waiting time. Overall, the service reallocation matches high-capacity modes to high-demand corridors while using flexible SAV services for lower-density areas.

Table 3. Result comparison between baseline case and optimal solution.

	Metrics	Baseline	First iteration best	Percentage change over baseline	Global best	Percentage change over baseline
Total	Served demand	930,742	1,161,785	24.8%	1,240,992	33.3%
	Active routes	274	265	-3.3%	108	-60.6%
Peak-hour	Served demand (per hour)	120,377	125,122	3.9%	135,020	12.2%
	Total frequency (per hour)	1677	1159	-30.9%	1131	-32.6%
	Metro rail	98	67	-31.4%	97	-1.1%
	Suburban rail	34	27	-20.9%	32	-5.0%

	Metrics	Baseline	First iteration best	Percentage change over baseline	Global best	Percentage change over baseline
	Metro bus	1011	757	-25.2%	911	-9.9%
	Suburban bus	534	309	-42.2%	91	-83.0%
	Median route frequency (per hour)	4.1	3.6	-11.1%	11.0	170.3%
	Metro rail	12.2	9.6	-21.4%	17.7	44.3%
	Suburban rail	3.1	2.4	-20.3%	2.2	-28.6%
	Metro bus	8.2	6.8	-16.3%	13.2	61.9%
	Suburban bus	4.1	2.2	-46.6%	4.6	13.9%
	SAV feeder fleet size	0	5,000		5,000	
	SAV feeder waiting time (min)	N/A	14.2		14.4	
	SAV feeder usage out of all transit riders	N/A	15.4%		14.4%	
Non-peak	Served demand (per hour)	18,953	37,369	97.2%	39,170	106.7%
	Total frequency (per hour)	833	557	-33.1%	304	-63.5%
	Metro rail	49	37	-23.8%	20	-58.8%
	Suburban rail	11	13	15.8%	16	46.3%
	Metro bus	506	387	-23.5%	255	-49.6%
	Suburban bus	267	120	-55.1%	13	-95.2%
	Median route frequency (per hour)	2.0	2.2	6.6%	3.0	47.6%
	Metro rail	6.1	5.8	-4.5%	4.9	-19.4%
	Suburban rail	1.0	2.2	114.8%	2.8	171.1%
	Metro bus	4.1	2.7	-34.3%	2.5	-38.2%
	Suburban bus	2.0	1.5	-27.6%	3.4	67.8%
	SAV feeder fleet size	0	5,000		5,000	
	SAV feeder waiting time (min)	N/A	4.8		5.9	
	SAV feeder usage out of all transit riders	N/A	28.8%		35.4%	

Figure 5 illustrates the optimized transit networks at peak and off-peak hours, revealing the prevailing hub-and-spoke network of Chicago. Traditional transit modes maintain strong presence in the urban core and along major corridors within and outside the city, while SAVs are deployed to serve areas particularly outside the city center where traditional transit services are less efficient. The maps demonstrate how the reduction in suburban bus routes is compensated by increased rail and metro bus frequencies in core areas. This spatial redistribution of services appears to better match the demand patterns, while SAV helps to maintain accessibility across the service area.

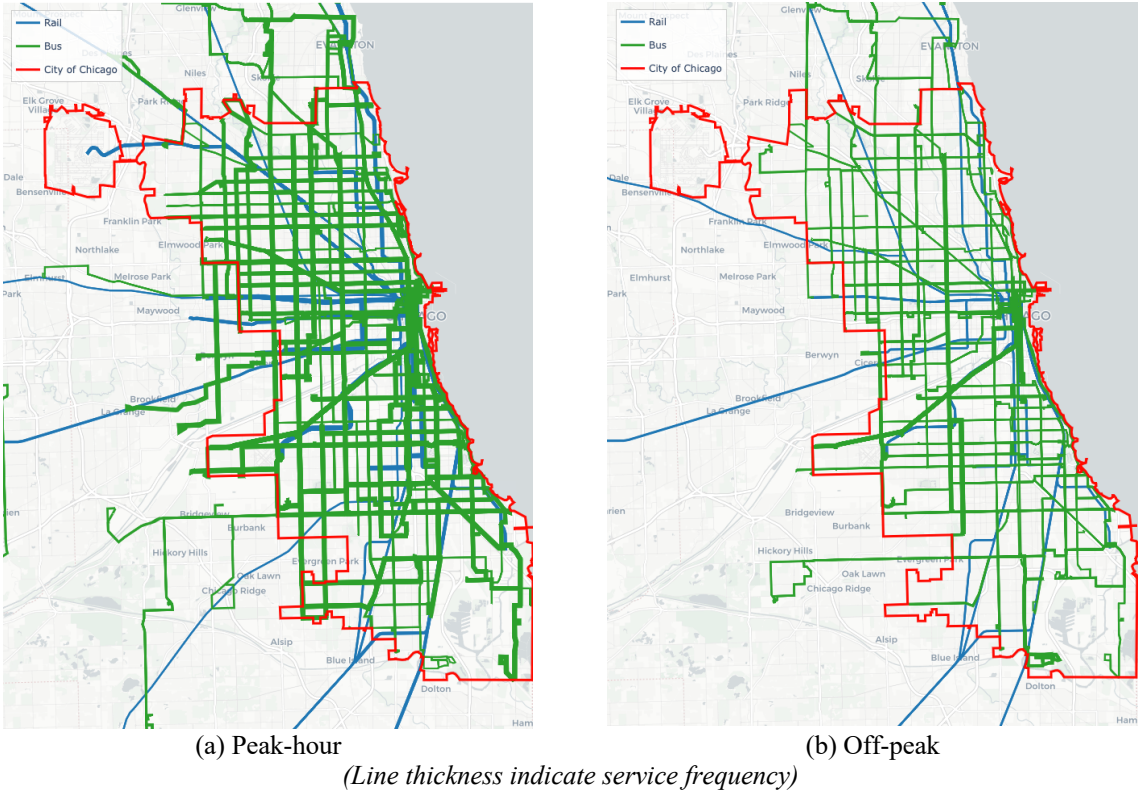


Figure 5. Transit routes in the optimal result.

5. CONCLUSION

5.1. Summary

This paper presents a comprehensive framework for jointly optimizing transit service frequency and SAV fleet size in multimodal networks. The proposed methodology addresses several key challenges in transit system planning through: (1) formulation of the joint optimization problem incorporating mode choice and route selection, (2) development of an efficient hybrid solution approach combining PSO with NLP in the complex non-convex solution space, and (3) implementation of practical approximation models for SAMS performance and user behavior.

The computational results from the Chicago metropolitan area case study demonstrate the framework's effectiveness in real-world applications. The hybrid PSO-NLP solution approach proves effective, demonstrating the value of combining global exploration with local optimization in addressing complex transit network problems. The approximation models

enable efficient evaluation of solutions without compromising the quality of the results. The optimal solution achieves a 33.3% increase in total transit ridership compared to the baseline case, with particularly strong improvements in off-peak hours (106.7%). This improvement is achieved through strategic reallocation of resources, including concentration of traditional transit services in high-demand corridors and strategic deployment of SAV feeders in lower-density areas. SAMS integration proved critical to this ridership increase, with SAV feeders contributing to 14.4% of peak-hour trips and 35.4% of off-peak trips, helping to cover low-demand areas with lower operating costs than traditional transit modes.

From a practical perspective, this research provides several important insights for transit agencies. While SAV integration can significantly improve system efficiency when strategically deployed, careful consideration must be given to equity implications. SAVs facilitate service provision in larger areas with lower costs than current demand-responsive transit. Meanwhile, the current model's uniform treatment of SAV fleet allocation across zones may need refinement to ensure equitable service distribution, particularly in underserved communities where first/last mile connectivity is crucial. Besides, any changes in essential transit services, particularly involving new service mode like SAV feeders, benefits from community engagement and careful balance of operational efficiency, public service obligations, and community expectations.

5.2. Limitations and Future Research

The framework's limitations suggest several directions for future research. First, more sophisticated route choice modeling, e.g., hyperpath, can be integrated in the framework. Second, while this paper demonstrates the effectiveness of combining global search with NLP using PSO, future research could explore how different metaheuristics perform within this hybrid framework for various problem instances and network configurations. The choice of metaheuristic may depend on specific problem characteristics such as network size, demand patterns, and computational resources. Third, the effects of transit service and SAMS adjustment on road network congestion can be modeled to reflect the changes on journey time. Fourth, the framework can be integrated into comprehensive transit network redesign procedures (Ng et al., 2024b). Fifth, zonal design of SAV feeder services (such as zone-specific fleet size optimization and waiting time targets), based on local demand patterns, demographics, and existing transit accessibility, would enable more nuanced service design that better addresses equity concerns while maintaining operational efficiency. Lastly, more detailed modeling of mode choice behavior with point-to-point and feeder SAMS are necessary to include better understanding of user preferences, willingness to transfer, and sensitivity to waiting times across different demographic groups and trip purposes.

These advancements would further strengthen the framework's applicability to real-world transit planning challenges. The model can be applied in more scenarios, e.g., budget increase to determine potential ridership capture, or equity-focused service design to ensure fair distribution of benefits across communities. Additionally, future work could explore fleet pooling between SAMS feeders and point-to-point services and the overall integration with Mobility-as-a-Service platforms.

The methodology presented here provides a foundation for transit agencies to make informed decisions about service design and resource allocation in the era of autonomous vehicles. As cities continue to explore innovative transit solutions, this framework offers a practical

approach to optimizing multimodal systems while maintaining service quality and operational efficiency.

REFERENCES

- Aksoy, İ.C., Mutlu, M.M., 2024. Comparing the performance of metaheuristics on the Transit Network Frequency Setting Problem. *Journal of Intelligent Transportation Systems* 1–20. <https://doi.org/10.1080/15472450.2024.2392722>
- Alonso-Mora, J., Samaranayake, S., Wallar, A., Frazzoli, E., Rus, D., 2017. On-demand high-capacity ride-sharing via dynamic trip-vehicle assignment. *PNAS* 114, 462–467. <https://doi.org/10.1073/pnas.1611675114>
- Auld, J., Hope, M., Ley, H., Sokolov, V., Xu, B., Zhang, K., 2016. POLARIS: Agent-based modeling framework development and implementation for integrated travel demand and network and operations simulations. *Transportation Research Part C: Emerging Technologies* 64, 101–116. <https://doi.org/10.1016/j.trc.2015.07.017>
- Bertsimas, D., Sian Ng, Y., Yan, J., 2020. Joint Frequency-Setting and Pricing Optimization on Multimodal Transit Networks at Scale. *Transportation Science* 54, 839–853. <https://doi.org/10.1287/trsc.2019.0959>
- Blank, J., Deb, K., 2020. pymoo: Multi-Objective Optimization in Python. *IEEE Access* 8, 89497–89509.
- Boeing, G., 2024. Modeling and Analyzing Urban Networks and Amenities with OSMnx.
- Byrd, R.H., Nocedal, J., Waltz, R.A., 2006. Knitro: An integrated package for nonlinear optimization. *Large-scale nonlinear optimization* 35–59.
- Ceder, A., 2016. *Public Transit Planning and Operation: Modeling, Practice and Behavior*, Second Edition. CRC Press.
- Ceder, A., 1984. Bus frequency determination using passenger count data. *Transportation Research Part A: General* 18, 439–453. [https://doi.org/10.1016/0191-2607\(84\)90019-0](https://doi.org/10.1016/0191-2607(84)90019-0)
- Chicago Metropolitan Agency for Planning, 2023. *Activity-Based Model (ABM) Calibration and Validation Report*.
- Durán-Micco, J., Vansteenwegen, P., 2022. A survey on the transit network design and frequency setting problem. *Public Transp* 14, 155–190. <https://doi.org/10.1007/s12469-021-00284-y>
- Engelhardt, R., Dandl, F., Syed, A.-A., Zhang, Y., Fehn, F., Wolf, F., Bogenberger, K., 2022. FleetPy: A Modular Open-Source Simulation Tool for Mobility On-Demand Services. <https://doi.org/10.48550/arXiv.2207.14246>
- Furth, P.G., Wilson, N.H.M., 1981. *Setting Frequencies on Bus Routes: Theory and Practice*. *Transportation Research Record*.
- Gkiotsalitis, K., Cats, O., 2022. Optimal frequency setting of metro services in the age of COVID-19 distancing measures. *Transportmetrica A: Transport Science* 18, 807–827. <https://doi.org/10.1080/23249935.2021.1896593>
- Hyland, M., Mahmassani, H.S., 2018. Dynamic autonomous vehicle fleet operations: Optimization-based strategies to assign AVs to immediate traveler demand requests. *Transportation Research Part C: Emerging Technologies* 92, 278–297. <https://doi.org/10.1016/j.trc.2018.05.003>
- Ibarra-Rojas, O.J., Delgado, F., Giesen, R., Muñoz, J.C., 2015. Planning, operation, and control of bus transport systems: A literature review. *Transportation Research Part B: Methodological* 77, 38–75. <https://doi.org/10.1016/j.trb.2015.03.002>
- Iliopoulou, C., Kepaptsoglou, K., Vlahogianni, E., 2019. Metaheuristics for the transit route network design problem: a review and comparative analysis. *Public Transp* 11, 487–521. <https://doi.org/10.1007/s12469-019-00211-2>
- Jiang, Y., Rasmussen, T.K., Nielsen, O.A., 2022. Integrated Optimization of Transit Networks with Schedule- and Frequency-Based Services Subject to the Bounded Stochastic User Equilibrium. *Transportation Science* 56, 1452–1468. <https://doi.org/10.1287/trsc.2022.1148>

- Kennedy, J., Eberhart, R., 1995. Particle swarm optimization, in: Proceedings of ICNN'95 - International Conference on Neural Networks. Presented at the Proceedings of ICNN'95 - International Conference on Neural Networks, pp. 1942–1948 vol.4. <https://doi.org/10.1109/ICNN.1995.488968>
- Levin, M.W., Odell, M., Samarasena, S., Schwartz, A., 2019. A linear program for optimal integration of shared autonomous vehicles with public transit. *Transportation Research Part C: Emerging Technologies* 109, 267–288. <https://doi.org/10.1016/j.trc.2019.10.007>
- Liu, Y., Ouyang, Y., 2021. Mobility service design via joint optimization of transit networks and demand-responsive services. *Transportation Research Part B: Methodological* 151, 22–41. <https://doi.org/10.1016/j.trb.2021.06.005>
- Luo, Q., Samaranyake, S., Banerjee, S., 2021. Multimodal mobility systems: joint optimization of transit network design and pricing, in: Proceedings of the ACM/IEEE 12th International Conference on Cyber-Physical Systems. Presented at the ICCPS '21: ACM/IEEE 12th International Conference on Cyber-Physical Systems, ACM, Nashville Tennessee, pp. 121–131. <https://doi.org/10.1145/3450267.3450540>
- Martínez, H., Mauttone, A., Urquhart, M.E., 2014. Frequency optimization in public transportation systems: Formulation and metaheuristic approach. *European Journal of Operational Research* 236, 27–36. <https://doi.org/10.1016/j.ejor.2013.11.007>
- Militão, A.M., Tirachini, A., 2021. Optimal fleet size for a shared demand-responsive transport system with human-driven vs automated vehicles: A total cost minimization approach. *Transportation Research Part A: Policy and Practice* 151, 52–80. <https://doi.org/10.1016/j.tra.2021.07.004>
- Mo, B., Cao, Z., Zhang, H., Shen, Y., Zhao, J., 2021. Competition between shared autonomous vehicles and public transit: A case study in Singapore. *Transportation Research Part C: Emerging Technologies* 127, 103058. <https://doi.org/10.1016/j.trc.2021.103058>
- Narayanan, S., Chaniotakis, E., Antoniou, C., 2020. Shared autonomous vehicle services: A comprehensive review. *Transportation Research Part C: Emerging Technologies* 111, 255–293. <https://doi.org/10.1016/j.trc.2019.12.008>
- Newell, G.F., 1971. Dispatching Policies for a Transportation Route. *Transportation Science* 5, 91–105. <https://doi.org/10.1287/trsc.5.1.91>
- Ng, M.T.M., Dandl, F., Mahmassani, H.S., Bogenberger, K., 2024a. Semi-on-Demand Hybrid Transit Route Design with Shared Autonomous Mobility Services. Presented at the 103rd Transportation Research Board Annual Meeting, Washington, D.C.
- Ng, M.T.M., Engelhardt, R., Dandl, F., Volakakis, V., Mahmassani, H.S., Bogenberger, K., 2025a. Semi-on-Demand Off-Peak Transit Services with Shared Autonomous Vehicles - Service Planning, Simulation, and Analysis in Munich, Germany, in: 104th Transportation Research Board Annual Meeting. arXiv, Washington, D.C. <https://doi.org/10.48550/arXiv.2408.10547>
- Ng, M.T.M., Mahmassani, H.S., 2022. Autonomous Minibus Service With Semi-on-Demand Routes in Grid Networks. *Transportation Research Record* 03611981221098660. <https://doi.org/10.1177/03611981221098660>
- Ng, M.T.M., Mahmassani, H.S., Verbas, Ö., Cokyasar, T., Engelhardt, R., 2024b. Redesigning large-scale multimodal transit networks with shared autonomous mobility services. *Transportation Research Part C: Emerging Technologies* 104575. <https://doi.org/10.1016/j.trc.2024.104575>
- Ng, M.T.M., Tong, D., Mahmassani, H.S., Verbas, O., Cokyasar, T., 2025b. Joint Optimization of Pattern, Headway, and Fleet Size of Multiple Urban Transit Lines with Perceived Headway Consideration and Passenger Flow Allocation, in: 104th Transportation Research Board Annual Meeting. arXiv, Washington, D.C. <https://doi.org/10.48550/arXiv.2409.19068>
- Pinto, H.K.R.F., Hyland, M.F., Mahmassani, H.S., Verbas, I.Ö., 2020. Joint design of multimodal transit networks and shared autonomous mobility fleets. *Transportation Research Part C: Emerging Technologies, ISTTT 23 TR_C-23rd International Symposium on Transportation and Traffic Theory (ISTTT 23)* 113, 2–20. <https://doi.org/10.1016/j.trc.2019.06.010>
- Schmidt, M., Schöbel, A., 2024. Planning and Optimizing Transit Lines. <https://doi.org/10.48550/arXiv.2405.10074>
- Verbas, İ.Ö., Frei, C., Mahmassani, H.S., Chan, R., 2015a. Stretching resources: sensitivity of optimal bus frequency allocation to stop-level demand elasticities. *Public Transp* 7, 1–20. <https://doi.org/10.1007/s12469-013-0084-6>

- Verbas, İ.Ö., Mahmassani, H.S., 2015. Exploring trade-offs in frequency allocation in a transit network using bus route patterns: Methodology and application to large-scale urban systems. *Transportation Research Part B: Methodological, Optimization of Urban Transportation Service Networks* 81, 577–595. <https://doi.org/10.1016/j.trb.2015.06.018>
- Verbas, İ.Ö., Mahmassani, H.S., 2013. Optimal Allocation of Service Frequencies over Transit Network Routes and Time Periods: Formulation, Solution, and Implementation Using Bus Route Patterns. *Transportation Research Record* 2334, 50–59. <https://doi.org/10.3141/2334-06>
- Verbas, İ.Ö., Mahmassani, H.S., Hyland, M.F., 2015b. Dynamic Assignment-Simulation Methodology for Multimodal Urban Transit Networks. *Transportation Research Record* 2498, 64–74. <https://doi.org/10.3141/2498-08>
- Zhou, Y., Yang, H., Wang, Y., Yan, X., 2021. Integrated line configuration and frequency determination with passenger path assignment in urban rail transit networks. *Transportation Research Part B: Methodological* 145, 134–151. <https://doi.org/10.1016/j.trb.2021.01.002>

ACKNOWLEDGMENT

This material is based on work partially supported by the U.S. Department of Energy, Office of Science, under contract number DE-AC02-06CH11357. This report and the work described were sponsored by the U.S. Department of Energy (DOE) Vehicle Technologies Office (VTO) under the Transportation Systems and Mobility Tools Core Maintenance/Pathways to Net-Zero Regional Mobility, an initiative of the Energy Efficient Mobility Systems (EEMS) Program. Additional funding was provided by the Northwestern University Transportation Center. The computational experiments were supported in part through the computational resources and staff contributions provided for the Quest high performance computing facility at Northwestern University. The authors remain responsible for all findings and opinions presented in the paper. The contents do not necessarily reflect the views of the sponsoring organizations. Given the simplified assumptions used in the model, this study does not constitute any policy suggestion on current operations.